International Journal of Aeronautical and Space Sciences (2022) 23:980–991
https://doi.org/10.1007/s42405-022-00480-5

IJASS International Journal of Aeronautical and Space Sciences

ORIGINAL PAPER

Reentry Attitude Fault Tolerant Control for RLV Based on Adaptive Second-Order Nonsingular Fast Terminal Sliding Mode

Dakai Liu[1,2] · Sven K. Esche[2] · Mingang Wang[1] · Xiaofei Chang[1]

Received: 16 December 2021 / Revised: 24 April 2022 / Accepted: 12 May 2022 / Published online: 22 June 2022

Abstract
In this paper, a novel adaptive continuous nonsingular fast terminal sliding mode fault tolerant control scheme for reusable launch vehicles (RLVs) is proposed. This scheme was designed to counteract the modeling uncertainties, external disturbances and actuator faults during the reentry phase. First, an attitude dynamics model for the reentry of RLVs is built. Then, with feedback linearization, a second-order attitude tracking error model is derived. Subsequently, based on the traditional discontinuous nonsingular fast terminal sliding manifold (NFTSM), a second-order continuous NFTSM-based control strategy is developed to achieve a fast and accurate attitude tracking in the presence of uncertainties, disturbances and actuator faults. Compared with the existing NFTSM-based control strategies, the proposed control law guarantees higher robustness and chattering reduction without introducing state or disturbance observers. Thus, the proposed control law has a more concise and simpler structure. Furthermore, it does not require prior knowledge of the upper bounds of the disturbances. While most of the existing control strategies based on the NFTSM tend to suffer large oscillations at the initial phase of the control process, the proposed control law eliminates these oscillations. Finally, simulations are carried out that demonstrate that the proposed control law has better robustness to disturbances and faults while creating less chattering than the exiting control laws.

Keywords RLV · Finite-time fault tolerant control · Nonsingular fixed-time terminal sliding mode · Adaptive gain · Higher order sliding mode control

1 Introduction

Reusable launch vehicles (RLVs) have attracted tremendous attention by researchers due to their excellent traits, such as low flight cost and reusability. They are expected to play an important role in military and civil applications in the future [1]. However, great challenge are encountered in the reentry phase, in which the vehicles suffer significant uncertainties, severe external disturbances and poor aerodynamic maneuverability [2]. Thus, rendering the control strategy more robust to the uncertainties, disturbances and actuator faults and causing it to stabilize more rapidly and accurately becomes an essential research topic.

Fault tolerant control (FTC) strategies are designed to maintain safe operating limits and to mitigate the effects of system/component malfunctions [3]. FTC for the reentry vehicle has been extensively studied in recent years, and many types of robust control approaches have been used as the basis for developing FTC [4]. The approaches include H_∞ control [5, 6], back-stepping control [7, 8], sliding mode control (SMC) [9, 10] and others. Among these approaches, the SMC is an attractive choice because of its useful properties, including superior robustness to disturbances, finite-time convergence and higher control precision, etc. The rotational equation for RLVs in the reentry phase is of second order. For stabilizing the second-order system, the terminal sliding manifold (TSM) is a suitable choice, since it has advantageous properties including fast and finite-time convergence [11, 12]. However, there exists a singularity problem for the early TSM methods. To overcome this problem, many researches on the non-singular TSM (NTSMC) have been carried out [13–16].In addition, the traditional TSM does not demonstrate uniform convergence speed when the system states are at different ranges from the equilibrium.

✉ Dakai Liu
dliu18@stevens.edu

[1] School of Astronautics, Northwestern Polytechnical University, Xi'an 710072, Shaanxi, China

[2] Department of Mechanical Engineering, Stevens Institute of Technology, Hoboken, NJ 07030, USA

Hence, the so-called fast TSM (FTSM) strategies were proposed to compensate for this shortcoming [17, 18]. In the FTSM, the convergence is rapid even when the states are far from the equilibrium. An advanced version of the FTSM is the fixed-time TSM, which drives the system to the origin in fixed time. In recent years, extensive research on the nonsingular fast/fixed-time TSM control (NFTSMC) has been conducted [19–21]. In particular, a singularity-free fixed time TSM structure that possesses a faster convergence speed and retains a higher control precision than its predecessors was proposed in [19].

On the other hand, in spite of the advances in the NFTSMC, the control laws proposed are always discontinuous. This can give rise to large undesirable chattering as was shown in the simulation tests in reference [19]. To solve this problem, saturation functions and boundary-layer functions were employed [22]. While the chattering is reduced by that, the system's trajectories are not constrained exactly on the sliding surface but rather to its vicinity. Consequently, the robustness of the controller is weakened. The designers still have to make the trade-off between the control accuracy and the chattering reduction. The approach to solve this dilemma is the higher order SMC strategy. However, the difficulty of designing a higher order NFTSMC lies in its special structure. Specifically, the derivative of the sliding manifold is an implicit function for the control law u [as is shown in Eq. (27)]. Moreover, the upper bounds of the disturbances and uncertainties are always assumed to be known a priori. However, they are not easily obtained in real applications. In addition, any overestimation of the disturbances leads to additional unwanted chattering. To resolve these two problems, two major types of methods have been studied recently. One resorts to a sliding manifold on the basis of the properties of the homogeneous system [23], which we will refer to as the homogeneity-based TSM (HBTSM) here. The derivative of such a terminal sliding manifold is an explicit function for the control u. Based on the HBTSM, an adaptive continuous nonsingular control law can be developed [24–27]. In [24], the equivalent control based adaptive super-twisting algorithm was combined with the HBTSM, which results in a continuous controller and mitigates the chattering. In [25, 26, 28], the multivariable version of the HBTSM was established and used to develop a continuous fault tolerant control algorithm. However, compared with the NFTSMC, the HBTSM has several disadvantages. For instance, for the HBTSM, it is hard to estimate the upper bound for the convergence time and the property of fast/fixed-time convergence vanishes. Another type of method is to use a disturbance observer, so that the effect of disturbances can be offset by their estimation [27, 29–33]. Without the influence of the disturbances, the discontinuous part (sign function) in the control law can be removed. However, the introduction of an observer increases the redundancy and complexity of the controller. Considering the shortcomings of the above methods, some researchers have made attempts to develop a continuous NFTSMC without the usage of an observer. In [34], a higher order version of the NFTSMC was proposed by combining a super-twisting SMC. However, the stability of the system has not been proved in this design and the stability of the system may not be guaranteed under all conditions [35].

Moreover, due to the unique structure of the traditional discontinuous NFTSMC, the magnitude of its output value during the initial stage of the control process is sensitive to the change of the disturbance value [19]. As a consequence, the initial control signal magnitude increases dramatically when the disturbance becomes slightly larger. This effect tends to give rise to large oscillations, which can lead to instability when there exists control saturation.

Motivated by the aforementioned problems, a novel adaptive second-order nonsingular fast terminal sliding mode controller (A2-NFTSMC) is proposed and applied to fault tolerant control of the RLV attitude in this paper. The main contributions are summarized as follows:

a) The proposed controller is developed on the basis of the well-researched NFTSMC, instead of the HBTSM. Thus, the properties of fast/fixed-time convergence and easy estimation of convergence time are inherited from the NFTSMC.
b) The proposed controller represents a second-order sliding mode algorithm. As a result, the chattering is greatly attenuated compared with the existing discontinuous NFTSMC without sacrificing the algorithm's accuracy and robustness to disturbances and faults. In addition, the proposed controller does not rely on observers to estimate the external disturbances. Therefore, the structure of the controller is simpler and more concise.
c) Unlike most of the existing control laws based on the NFTSMC, the proposed controller does not require any prior knowledge of the external disturbances, modeling uncertainties or actuator faults. In addition, the shortcoming of the traditional NFTSMC that its output magnitude is sensitive to the change of the disturbance value is overcome in the proposed control strategy. Consequently, the hazard of introducing large oscillations during the initial stage of the control process is eliminated.

This paper is organized as follows. Section 1 gives an introduction of this research. Section 2 presents the modeling of the RLV dynamics during the reentry phase and the statement of the control problem. Section 3 is dedicated to the proposed adaptive second-order nonsingular fast terminal sliding mode controller design. Section 4 provides simulation tests to demonstrate the efficacy of the proposed method. The conclusions are given in Sect. 5.

Notation 1: In this paper, the following notations are used. $\|\cdot\|$ denotes the Euclidean norm of vectors or the induced norm of matrices.

Notation 2: For any vector $x = [x_1, x_2, \cdots, x_n]^T$ and positive constant r, denote $sign^r(x) = \left[|x_1|^r sign(x_1), \quad |x_2|^r sign(x_2), \quad \cdots, |x_n|^r sign(x_n)\right]$.

2 Dynamics Modeling and Problem Statement

During the reentry phase, the motion of RLVs can be decomposed into rotational motion and translational motion. The equations of rotational motion are described as [4, 36]

$$\begin{aligned}
\dot{p} &= \frac{J_{zz}M_x}{J_{xx}J_{zz}-J_{xz}^2} + \frac{J_{xz}M_z}{J_{xx}J_{zz}-J_{xz}^2} + \frac{(J_{xx}-J_{yy}+J_{zz})J_{xz}}{J_{xx}J_{zz}-J_{xz}^2}pq \\
&\quad + \frac{(J_{yy}-J_{zz})J_{zz}-J_{xz}^2}{J_{xx}J_{zz}-J_{xz}^2}qr, \\
\dot{q} &= \frac{M_x}{J_{yy}} + \frac{J_{xz}}{J_{yy}}(r^2-p^2) + \frac{J_{zz}-J_{xx}}{J_{yy}}pr, \\
\dot{r} &= \frac{J_{xz}M_x}{J_{xx}J_{zz}-J_{xz}^2} + \frac{J_{xx}M_z}{J_{xx}J_{zz}-J_{xz}^2} + \frac{(J_{xx}-J_{yy})J_{xx}+J_{xz}^2}{J_{xx}J_{zz}-J_{xz}^2}pq \\
&\quad + \frac{(J_{yy}-J_{xx}-J_{zz})J_{xz}}{J_{xx}J_{zz}-J_{xz}^2}qr,
\end{aligned} \tag{1}$$

$$\begin{aligned}
\dot{\alpha} &= -p\cos\alpha\tan\beta + q - r\sin\alpha\tan\beta \\
&\quad + \frac{\sin\sigma}{\cos\beta}\big[\dot{\psi}\cos\gamma - \dot{\phi}\sin\psi\sin\gamma \\
&\quad + (\dot{\theta}+\omega_e)(\cos\phi\cos\psi\sin\gamma - \sin\phi\cos\gamma)\big] \\
&\quad - \frac{\cos\sigma}{\cos\beta}\big[\dot{\gamma} - \dot{\phi}\cos\psi - (\dot{\theta}+\omega_e)\cos\phi\sin\psi\big], \\
\dot{\beta} &= p\sin\alpha - r\cos\alpha + \sin\sigma\big[\dot{\gamma} - \dot{\phi}\cos\psi - (\dot{\theta}+\omega_e)\cos\phi\sin\psi\big] \\
&\quad \cos\sigma\big[\dot{\psi}\cos\gamma - \dot{\phi}\sin\psi\sin\gamma \\
&\quad + (\dot{\theta}+\omega_e)(\cos\phi\cos\psi\sin\gamma - \sin\phi\cos\gamma)\big], \\
\dot{\sigma} &= -p\cos\alpha\cos\beta - q\sin\beta - r\sin\alpha\cos\beta + \dot{\alpha}\sin\beta - \dot{\psi}\sin\gamma \\
&\quad - \dot{\phi}\sin\psi\cos\gamma + (\dot{\theta}+\omega_e)(\cos\phi\cos\psi\cos\gamma - \sin\phi\sin\gamma),
\end{aligned} \tag{2}$$

where p, q, r are the roll, pitch and yaw angular rates; α, β, σ represent the angle of attack, the sideslip angle and bank angle; γ is the flight path angle; ψ is the heading angle; ω_e is the Earth's angular speed; θ and ϕ are the longitude and latitude; J_{ij} $(i = x, y, z;\ j = x, y, z)$ is the moment of inertia; M_x, M_y, M_z are the roll, pitch yaw moments, respectively.

Since the rotational motions of RLVs are much faster than their translational motions, the time derivatives of both the position and the velocity are considered to be negligible with respect to the rotational motion. Equations (1) and (2) can be simplified as [37]

$$\dot{\Omega} = R\omega + \Delta f, \tag{3}$$

$$\dot{\omega} = -J^{-1}\omega^{\times}J\omega + J^{-1}M + \Delta d, \tag{4}$$

where $M = [M_x\ M_y\ M_z]^T$, $\Omega = [\alpha\ \beta\ \sigma]^T$, and $\omega = [p\ q\ r]^T$; $\Delta f = [\Delta f_x\ \Delta f_y\ \Delta f_z]^T$ is the bounded differentiable unmatched disturbance vector caused by simplified modeling; $\Delta d \in \Re^3$ is the bounded unknown disturbance vector caused by model uncertainty and external disturbances. J, R, $\omega^{\times} \in \Re^{3\times3}$ are the nominal inertia matrix, the coordinate transformation matrix and the skew–symmetric matrix operator on vector ω, respectively. They are defined as follows:

$$\begin{aligned}
J &= \begin{bmatrix} J_{xx} & 0 & -J_{xz} \\ 0 & J_{yy} & 0 \\ -J_{xz} & 0 & J_{zz} \end{bmatrix}, \quad \omega^{\times} = \begin{bmatrix} 0 & -r & q \\ r & 0 & -p \\ -q & p & 0 \end{bmatrix} \\
R &= \begin{bmatrix} -\cos\alpha\tan\beta & 1 & -\sin\alpha\tan\beta \\ \sin\alpha & 0 & -\cos\alpha \\ -\cos\alpha\cos\beta & -\sin\alpha & -\sin\alpha\cos\beta \end{bmatrix},
\end{aligned} \tag{5}$$

where Δd can be expressed as $\Delta d = J^{-1}[-\Delta J\dot{\omega} - \omega^{\times}\Delta J\omega + \Delta M]$, where $\Delta J \in \Re^{3\times3}$ is the uncertain part of the inertia matrix and $\Delta M \in \Re^3$ is a vector of unknown external disturbances.

To further include possible actuator faults, Eq. (4) can be expressed as

$$\begin{aligned}
\dot{\omega} &= -J^{-1}\omega^{\times}J\omega + J^{-1}[\Lambda M + F_{\delta}] + \Delta d \\
&= -J^{-1}\omega^{\times}J\omega + J^{-1}M + J^{-1}[(\Lambda - I)M + F_{\delta}] + \Delta d,
\end{aligned} \tag{6}$$

where vector $\Lambda = diag[\Lambda_x\ \Lambda_y\ \Lambda_z]$ is the actuator effectiveness with $0 \le \Lambda_i \le 1$, $i = x, y, z$ and $F_{\delta} \in [F_{\delta_x}\ F_{\delta_y}\ F_{\delta_z}]$ is the actuator bias fault.

The aim of this paper is to design a continuous sliding mode controller such that the angle vector Ω tracks the guidance command $\Omega_{ref} = [\alpha_{ref}\ \beta_{ref}\ \sigma_{ref}]^T$ accurately in finite time in the presence of uncertainties Δf and disturbances Δd.

For the sake of the controller design, feedback linearization of the dynamic system is carried out first. Assume that $X_1 = \Omega - \Omega_{ref}$ and $X_2 = \dot{\Omega} - \dot{\Omega}_{ref}$, which denote the tracking errors of the attitude angles and the angular rates, respectively. By differentiating X_1 and X_2, we obtain

$$\dot{X}_1 = X_2, \tag{7}$$

$$\dot{X}_2 = F + GM + \Delta D, \tag{8}$$

where $X_1 = [x_{1x}\ x_{1y}\ x_{1z}]$, $X_2 = [x_{2x}\ x_{2y}\ x_{2z}]$; $G = RJ^{-1}$; $F = [F_x\ F_y\ F_z]$ is the known normal part of the system; the disturbance $\Delta D = [\Delta D_x\ \Delta D_y\ \Delta D_z]$ is the unknown part which is induced by uncertainties, disturbances and actuator faults. Here, F and ΔD can be expressed as

$$F = \left(\dot{R} - RJ^{-1}\omega^{\times}J\right)\omega - \ddot{\Omega}_{ref}, \tag{9}$$

$$\Delta D = RJ^{-1}[(\Lambda - I)M + F_{\delta}] + R\Delta d + \Delta\dot{f}. \tag{10}$$

Since, during the reentry phase, angle β is kept near 0, we have

$$\det(G) = \frac{\cos\beta - \sin\beta\tan\beta}{J_{xx}J_{zz} - J_{xz}^2} \approx \frac{1}{J_{xx}J_{zz} - J_{xz}^2} \neq 0. \tag{11}$$

Therefore, G^{-1} exists. Introducing a control vector $U = [u_x,\ u_y,\ u_z]$ and defining it as $U = GM$, Eq. (8) can be expressed as

$$\dot{X}_2 = F + U + \Delta D. \tag{12}$$

Assumption 1 [26]: It is assumed that uncertainty ΔD in (10) is differentiable and bounded with $\|\Delta D\| \leq L_1$; its derivative is also bounded with $\left\|\Delta\dot{D}\right\| \leq L_2$, where L_1 and L_2 are unknown positive constants.

Assumption 2 [26]: Assume that the condition $\left\|J^{-1}(\Lambda - I)J\right\| < 1$ holds.

Remark 1 Eq. (6) can be rewritten as

$$\begin{aligned}\dot{\omega} = &-J^{-1}\omega^{\times}J\omega + \left(I + J^{-1}(\Lambda - I)J\right)J^{-1}M \\ &+ J^{-1}F_{\delta} + \Delta d.\end{aligned} \tag{13}$$

In the second term in (13), i.e., the control term, $J^{-1}(\Lambda - I)J$ denotes the uncertain portion of the matrix and the identity matrix I represents the nominal portion. According to [38], for the nominal part of the control signal to dominate the uncertain part, condition $\left\|\left(J^{-1}(\Lambda - I)J\right)\cdot I^{-1}\right\| < 1$ must be satisfied.

3 Controller Design

3.1 Preliminaries

Lemma 1 [19] *Consider the following scalar system:*

$$\dot{y} = -l_1 sign^{m_1} y - l_2 sign^{m_2} y,\ \ y(0) = y_0, \tag{14}$$

where $l_1 > 0$, $l_2 > 0$, $m_1 \geq 1$ and $0 < m_2 < 1$. The equilibrium point of the above system is finite time stable, and the convergence time T is bounded by

$$T \leq T_{\max} = \frac{1}{l_1(m_1 - 1)} + \frac{1}{l_2(1 - m_2)}. \tag{15}$$

Remark 2 Note that the upper bound of convergence time does not depend on the initial value y_0. Then system (14) can be seen as being fixed-time stable [39].

Lemma 2 [40] (Jensen's inequality) *For a vector $v = [v_1\ v_2 \cdots v_n]$ with $v_i \geq 0$, there holds inequality.*

$$\left(\sum_{i=0}^{n} v_i^q\right)^{1/q} \leq \left(\sum_{i=0}^{n} v_i^p\right)^{1/p}, \tag{16}$$

if $0 < p < q$.

Lemma 3 [40] *For a continuous convex function f, if numbers v_1, $v_2 \cdots v_n$ are in its domain, then there holds inequality:*

$$f\left(\sum_{i=0}^{n} v_i/n\right) \leq \left(\sum_{i=0}^{n} f(v_i)\right)/n. \tag{17}$$

Lemma 4 *For a vector $v = [v_1\ v_2 \cdots v_n]$ with $v_i \geq 0$, it can be proven from Lemma 2 and Lemma 3 that there hold inequalities:*

$$\sum_{i=0}^{n} v_i \leq \left(\sum_{i=0}^{n} v_i^p\right)^{1/p}, \ \text{if } p < 1, \tag{18}$$

$$\sum_{i=0}^{n} v_i \leq n^{p-1}\left(\sum_{i=0}^{n} v_i^p\right)^{1/p}, \ \text{if } p > 1. \tag{19}$$

3.2 Design of Adaptive Second-Order Nonsingular Fast Terminal Sliding Mode Controller

In order for the angle vector Ω to track the guidance command Ω_{ref}, the controller to be designed should cause state vector X_1 in (7) to converge to the origin in finite time. Thus, in this section, a novel A2-NFTSMC that achieves this goal will be proposed. First, assume that state vector X_2 is obtainable. The terminal sliding manifold is chosen as [19]

$$\begin{aligned}S_i = &sign^{a_{1i}} x_{1i} + \frac{k_{2i}a_{2i}}{2a_{2i} - 1} sign^{2 - 1/a_{2i}}\left(x_{2i} + k_{1i} sign^{a_{1i}} x_{1i}\right), \\ &i = x,\ y,\ z,\end{aligned} \tag{20}$$

where control parameters $k_{1i} > 0$, $k_{2i} > 0$, $a_{2i} > 1$ and $1 < a_{1i} < 2 - 1/a_{2i}$ are preselected. Then, define $S = [S_x,\ S_y,\ S_z]$.

Theorem 1 *When the sliding manifold satisfies $S = 0$, state vectors X_1 and X_2 converge to the origin in fixed time, and the upper bound for the convergence time for each pair of their elements is*

$$T_{si} = \frac{1}{\bar{k}_{1i}(\bar{a}_{1i} - 1)} + \frac{1}{\bar{k}_{2i}(1 - \bar{a}_{2i})}, \quad i = x, y, z,$$

where $k_{1i} = \bar{k}_{1i}, \bar{k}_{2i} = ((2a_{2i} - 1)/k_{2i}a_{2i})^{a_{2i}/(2a_{2i}-1)}, \bar{a}_{1i} = a_{1i}$ *and* $\bar{a}_{2i} = a_{1i}a_{2i}/(2a_{2i} - 1)$.

Proof As $\dot{X}_1 = X_2$, when $S = 0$, Eq. (20) can be transformed into

$$\dot{x}_{1i} = -\bar{k}_{1i} sign^{\bar{a}_{1i}} x_{1i} - \bar{k}_{2i} sign^{\bar{a}_{2i}} x_{1i}, \quad i = x, y, z, \quad (21)$$

By Lemma 1, we can obtain that the upper bound of the convergence time for each x_{1i} equals T_{si}. Then, as x_{1i} is stable and constant, the state x_{2i} also converges to the origin correspondingly.

To drive the sliding manifold S to the origin in finite time while resisting disturbance ΔD in the meantime, an adaptive continuous control law is presented as

$$\begin{aligned} u_i = &-F_i - k_{1i}a_{1i}\,|x_{1i}|^{a_{1i}-1}\left(\frac{\phi_i}{k_{1i}} + x_{2i}\right) \\ &- k_{3i} sign^{c_1}(S_i) - k_{4i} sign^{c_2}(S_i) + v_i, \end{aligned} \quad (22)$$

$$\dot{v}_i = -r_i v_i - k_{di} sign(\chi_i), \quad i = x, y, z, \quad (23)$$

with

$$\begin{aligned} \phi_i = &\frac{1}{k_{2i}} sign^{1/a_{2i}}(x_{2i} + k_{1i} sign^{a_{1i}} x_{1i}) \\ &+ \frac{k_{1i}a_{2i}}{2a_{2i} - 1}(x_{2i} + k_{1i} sign^{a_{1i}} x_{1i}), \end{aligned} \quad (24)$$

and adaptive gain k_{di} chosen as

$$\dot{k}_{di} = \begin{cases} l_{0i}\left(|S_i|^{m_{1i}} + |S_i|^{m_{2i}}\right), & |S_i| > \varepsilon_0 \\ 0, & |S_i| \le \varepsilon_0 \end{cases} \quad (25)$$

where $\chi_i = v_i + \Delta D_i; k_{3i}, k_{4i}, r_i, l_{0i}, \gamma_0$ and ε_0 are preselected positive parameters; parameters c_1, c_2, m_{1i}, m_{2i} are chosen as $0 < c_1 < 1, c_2 > 1, 0 < m_{1i} < 1, m_{2i} > 1$. We can note that, according to Eq. (23), $sign(\chi_i)$ is required to implement the control law. How to obtain $sign(\chi_i)$ is explained Remark 3.

Theorem 2 *Consider the dynamic system of Eqs. (7) and (8), where the disturbance vector ΔD satisfies Assumption 1. If the controller is designed as in (22) to (25), then there exists a finite time in which the state vectors X_1 and X_2 converge to the origin.*

Proof In the following proof, subscript i is used to represent the three different channels x, y and z. Define a Lyapunov function

$$V_0 = \frac{1}{2} S^T S. \quad (26)$$

By differentiating function V_0 and taking into account the control U in (22), we obtain

$$\begin{aligned} \dot{V}_0 &= \sum_{i=x,y,z} S_i\left(a_{1i}|x_{1i}|^{a_{1i}-1}x_{2i} + \psi_i(\dot{x}_{2i} + a_{1i}k_{1i}|x_{1i}|^{a_{1i}-1}x_{2i})\right) \\ &= \sum_{i=x,y,z} S_i(a_{1i}|x_{1i}|^{a_{1i}-1}x_{2i} \\ &\quad + \psi_i(F_i + u_i + \Delta D_i + a_{1i}k_{1i}|x_{1i}|^{a_{1i}-1}x_{2i})) \\ &= \sum_{i=x,y,z} S_i(a_{1i}|x_{1i}|^{a_{1i}-1}x_{2i} + \psi_i(-a_{1i}|x_{1i}|^{a_{1i}-1}\phi_i \\ &\quad - k_{3i} sign^{c_1}(S_i) - k_{4i} sign^{c_2}(S_i) + v_i + \Delta D_i)), \end{aligned} \quad (27)$$

where $\psi_i = k_{2i}|x_{2i} + k_{1i} sign^{a_{1i}} x_{1i}|^{1-1/a_{2i}}$. Since, with regard to Eq. (24), there exists relation

$$\psi_i \phi_i = x_{2i} + k_{1i} S_i, \quad (28)$$

we further obtain

$$\begin{aligned} \dot{V}_0 &= \sum_{i=x,y,z} S_i\Big(-k_{1i}a_{1i}|x_{1i}|^{a_{1i}-1}S_i + \psi_i(-k_{3i} sign^{c_{1i}}(S_i) \\ &\quad -k_{4i} sign^{c_{2i}}(S_i) + v_i + \Delta D_i)\Big) \\ &\le \sum_{i=x,y,z} \Big(-k_{1i}a_{1i}|x_{1i}|^{a_{1i}-1}S_i^2 + \psi_i(-k_{3i}|S_i|^{c_{1i}} \\ &\quad -k_{4i}|S_i|^{c_{2i}}) + S_i\psi_i\chi_i\Big). \end{aligned} \quad (29)$$

We can notice that, as $\psi_i \ge 0$, the terms in (29) are all negative except for $S_i\psi_i\chi_i$. Now, prove that there exists a value of k_{di} for which χ_i converges to the origin in finite time. In view of Eq. (23), the derivative of χ_i is

$$\frac{\mathrm{d}\chi_i}{\mathrm{d}t} = -k_{di} sign(\chi_i) - r_i v_i + \Delta\dot{D}_i. \quad (30)$$

Consider a Lyapunov function candidate $V_{\chi_i} = \chi_i^2/2$. Combining with (30), we obtain the derivative of V_{χ_i}:

$$\begin{aligned} &\dot{V}_{\chi_i} = -k_{di}|\chi_i| - r_i v_i \chi_i + \Delta\dot{D}_i\chi_i \\ &\le -k_{di}|\chi_i| - r_i\chi_i^2 + \left|r_i\Delta D_i + \Delta\dot{D}_i\right||\chi_i| \\ &\le -k_{di}|\chi_i| - r_i\chi_i^2 + (r_iL_1 + L_2)|\chi_i|. \end{aligned} \quad (31)$$

If k_{di} satisfies the condition

$$k_{di} > r_iL_1 + L_2 + \varepsilon_i, \quad (32)$$

where ε_i is a predefined positive constant, Eq. (31) can be rewritten as

$$\dot{V}_{\chi i} \leq -\varepsilon_i \sqrt{V_{\chi i}} - r_i V_{\chi i}, \tag{33}$$

Thus, according to Lemma 1, $V_{\chi i}$ converges to the origin in finite time, which further establishes the finite-time convergence of χ_i.

In addition, since $a_{2i} > 1$, ψ_i is nonsingular. If both X_1 and X_2 are bounded, then S_i and ψ_i are also bounded. Therefore, the convergence of $S_i \psi_i \chi_i$ to 0 in finite time can be concluded. Then, since $(c_1 + 1)/2 < 1$ and $(c_2 + 1)/2 > 1$, in view of Lemma 4, we obtain

$$\begin{aligned}
\dot{V}_0 &\leq \sum_{i=x,\,y,\,z} \left(-k_{2i} a_{1i} |x_{1i}|^{a_{1i}-1} S_i^2 + \psi_i(-k_{3i}|S_i|^{c_1+1} - k_{4i}|S_i|^{c_2+1})\right) \\
&\leq \sum_{i=x,\,y,\,z} \psi_i \left(-k_{3i}\left(|S_i|^2\right)^{(c_1+1)/2} - k_{4i}\left(|S_i|^2\right)^{(c_2+1)/2}\right) \\
&\leq -2^{(c_1+1)/2} \min_{i=x,\,y,\,z}(\psi_i k_{3i}) V_0^{(c_1+1)/2} - 3^{(1-c_2^2)/4}\, 2^{(c_2+1)/2} \\
&\quad \min_{i=x,\,y,\,z}(\psi_i k_{4i}) V_0^{(c_2+1)/2}.
\end{aligned} \tag{34}$$

For the convenience of discussing the state of ψ_i, define two groups of areas Γ_{1i} and Γ_{2i}

$$\begin{aligned}
&\Gamma_{1i} = \{\psi_i \geq 1\},\ \ i = x,\ y,\ z, \\
&\Gamma_{2i} = \{\psi_i < 1\},\ \ i = x,\ y,\ z,
\end{aligned} \tag{35}$$

and $\kappa_i = x_{2i} + k_{1i} sign^{a_{1i}} x_{1i}$.

Case 1: When the states are all in the first group of areas Γ_{1i} $(i = x,\ y,\ z)$, it can be shown that

$$\begin{aligned}
\dot{V}_0 \leq &- \underbrace{2^{(c_1+1)/2} \min_{i=x,\,y,\,z}(k_{3i})}_{K_a} V_0^{(c_1+1)/2} \\
&- \underbrace{3^{(1-c_2^2)/4}\, 2^{(c_2+1)/2} \min_{i=x,\,y,\,z}(k_{4i})}_{K_b} V_0^{(c_2+1)/2}.
\end{aligned} \tag{36}$$

As $K_a > 0$ and $K_b > 0$, according to Lemma 1 and Theorem 1, states X_1 and X_2 can be driven to the origin in finite time.

Case 2: If the states are not all in the group of areas Γ_{1i} $(i = x,\ y,\ z)$, i.e., at least some states are in the second group of areas Γ_{2i}, there is a possibility that $\kappa_i = 0$. Here, it will be proved that the curve $\kappa_i = 0$ is not attractive unless $S_i = 0$. Supposing that $\kappa_i = 0$, then the derivative of κ_i is

$$\dot{\kappa}_i = -k_{3i} sign^{c_1}(S_i) - k_{4i} sign^{c_2}(S_i) + \chi_i. \tag{37}$$

As it has been shown that χ_i converges to 0 in finite time, $\dot{\kappa}_i > 0$ when $S_i < 0$ and $\dot{\kappa}_i < 0$ when $S_i > 0$. Hence, the states pass through Γ_{2i} and reach Γ_{1i} in finite time. As a result, the states converge to the origin in finite time no matter which areas the states are in.

The above proof was achieved under the premises that inequality (32) is satisfied and states X_1 and X_2 are bounded. Note that k_{di} is supposed to increase in accordance with Eq. (25) if (32) is not satisfied and, consequently, the sliding manifold does not converge to the origin. Therefore, condition (32) must be met in finite time. Thus, the divergence time for the states is also finite and the states X_1 and X_2 are bounded. In addition, since the sliding mode converges to the origin in finite time, adaptive gain k_{di} is also bounded.

The proof of theorem 2 further leads to the conclusion that with the controller designed as in (22)–(25), the angle vector Ω tracks the guidance command Ω_{ref} in finite time in the presence of disturbances, uncertainties and actuator faults as described in (3) and (6).

Remark 3 In view of the control law in (23), χ_i is not obtainable due to the unknown disturbance ΔD_i. Taking into account the control u_i in (22), $\dot{S}_i$ is obtained as

$$\begin{aligned}
\dot{S}_i = &-k_{2i} a_{1i} |x_{1i}|^{a_{1i}-1} S_i \\
&+ \psi_i(-k_{3i} sign^{c_{1i}}(S_i) - k_{4i} sign^{c_{2i}}(S_i) + \chi_i).
\end{aligned} \tag{38}$$

Since the curve $\kappa_i = 0$ is not an attractor except when $S_i = 0$, there is $\psi_i > 0$ almost all the time before the sliding manifold converges. Hence, resorting to the time delay method, $sign(\chi_i)$ can be achieved as follows [27]. Integrate both sides of (38) and define

$$\begin{aligned}
g(t) &= \int_0^t (\psi_i \chi_i) \mathrm{d}\tau \\
&= S_i + \int_0^t \Big(k_{2i} a_{1i} |x_{1i}|^{a_{1i}-1} S_i + \psi_i \\
&\quad \times \left(k_{3i} sign^{c_{1i}}(S_i) + k_{4i} sign^{c_{2i}}(S_i)\right)\Big) \mathrm{d}\tau.
\end{aligned} \tag{39}$$

There is $\psi_i \chi_i = \lim_{\tau \to 0}(g(t) - g(t-\tau))/\tau$, which further leads to

$$sign(\chi_i) = sign(g(t) - g(t-\tau)), \tag{40}$$

where τ is a short time delay.

Remark 4 According to the definition of k_{di} in (25), when $|S_i| > \varepsilon_0$, k_{di} increases until condition (32) is satisfied before the system states start to converge to the origin. With Eqs. (25) and (32), it can be deduced that the time interval of this process is finite and bounded by $(r_i L_1 + L_2 + \varepsilon_i) \big/ \left(l_{0i} |\varepsilon_0|^{m_{1i}} + l_{0i} |\varepsilon_0|^{m_{2i}}\right)$.

Remark 5 Note that in Eq. (27), $\dot{V}_0$ is an implicit function for control law u_i. Therefore, many higher order sliding mode

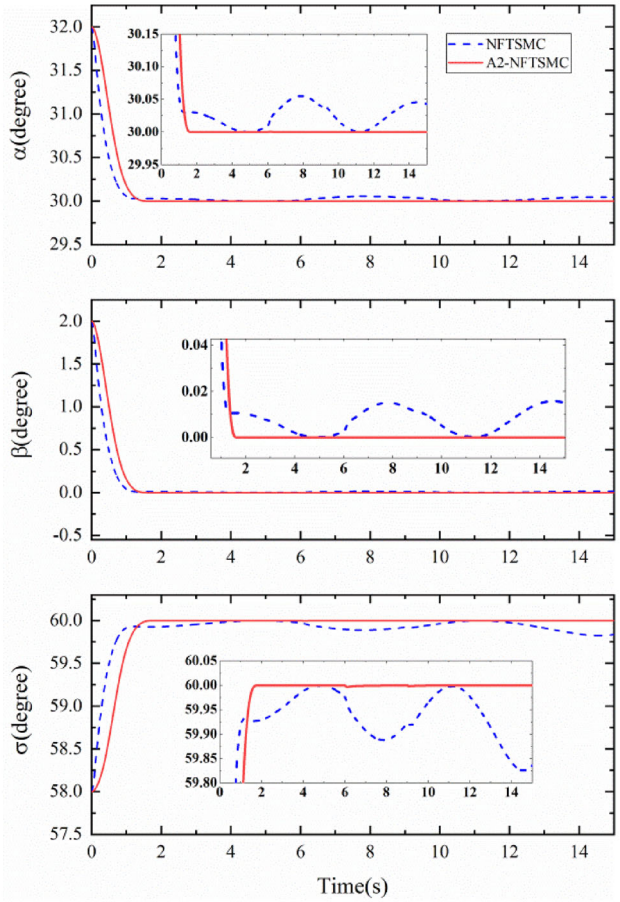

Fig. 1 Comparison of angle of attack, sideslip angle and bank angle between NFTSMC and proposed controller

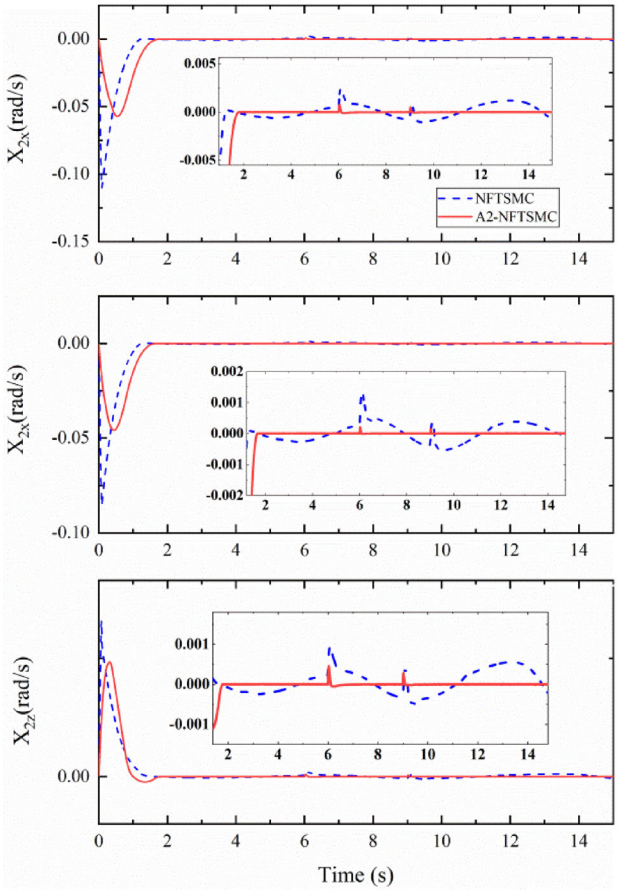

Fig. 2 Comparison of convergence of X_2 between NFTSMC and proposed controller

control strategies, such as the super-twisting algorithm, cannot be directly applied here. Although an attempt was made to combine a super-twisting control law with the NFTSMC in reference [34], there was no strict stability proof given and the system may not be stable under certain conditions [35]. The adaptive A2-NFTSMC strategy proposed in this paper represents a second-order sliding mode control law. It is an augmentation of the discontinuous version of the NFTSMC in [19]. Compared with the discontinuous one, the chattering is reduced, while the controller precision and robustness is guaranteed at the same time. As the gain k_{di} is adaptive, there is no need to know the upper bound of the disturbance. In addition, an accelerating term $-r_i v_i$ is injected in (23) and the convergence speed is increased.

Remark 6 Another benefit of the proposed adaptive second-order structure of u_i in (22) is its insensitivity to the change of the magnitude of the disturbance as long as the initial values of v_i are set to 0. The reason for this is that v_i tracks $-\Delta D_i$ rather fast without causing a large overshoot. However, for the traditional NFTSMC, a slight increase of the magnitude of the discontinuous term is amplified by the unique structure of NFTSMC, which further gives rise to a large overshoot (to be shown in the simulations below).

Remark 7 The design of this control strategy is partly motivated by reference [27]. Compared with the sliding manifold applied in [27], the sliding manifold selected in this paper (NFTSM) has advantageous features. The design of the control law in [27] is based on a sliding manifold with homogeneous property [23]. Although it was proven to be finite time convergent, the convergence time is hard to calculate. Meanwhile, compared with the NFTSM, not only has it faster converging speed than the other one and its convergence time is fixed instead of being only finite, but also its convergence time is easy to obtain according to Lemma 1.

4 Simulation

In this section, the results of two simulation tests are presented to demonstrate the performance of the proposed controller. In the first test, the traditional NFTSMC method

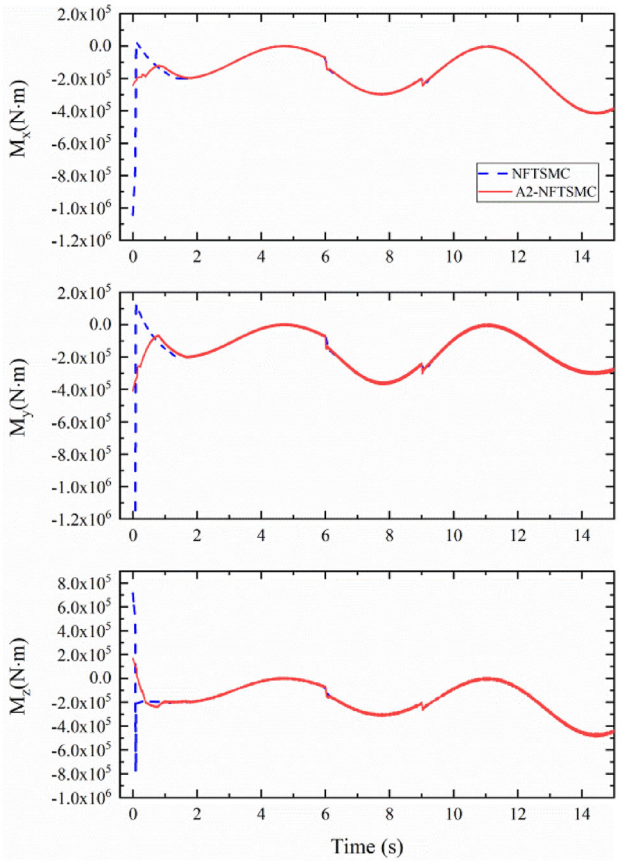

Fig. 3 Comparison of control torque between NFTSMC and proposed controller

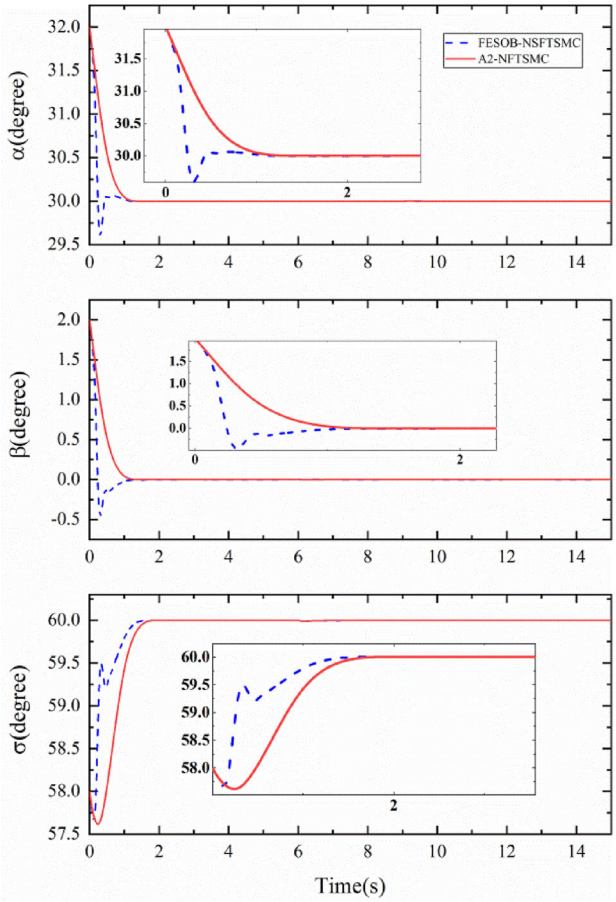

Fig. 4 Comparison of angle of attack, sideslip angle and bank angle between FESOB–NSFTSMC and proposed controller

in [19] is compared with the proposed one. The simulation test is similar to the ones described in [4, 36].

The parameters of the RLV in the test are as follows. The moments of inertia are $J_{xx} = 588791kg \cdot m^2$, $J_{xz} = 24242kg \cdot m^2$, $J_{yy} = 1303212kg \cdot m^2$ and $J_{zz} = 1534164kg \cdot m^2$. The system is subjected to the initial conditions $\alpha(0) = 32°$, $\beta(0) = 2°$, $\sigma(0) = 58°$, and $p(0) = q(0) = r(0) = 0°/s$. The guidance commands are set as $\alpha_{ref} = 30°$, $\beta_{ref} = 0°$ and $\sigma_{ref} = 60°$.

The external disturbance ΔM is set as

$$\Delta M = \begin{bmatrix} 1+\sin(t) \\ 1+\sin(t) \\ 1+\sin(t) \end{bmatrix} \times 10^5 N.m, \tag{41}$$

and the actuator faults are given as

$$F_\delta = \frac{1}{2} \times \begin{bmatrix} 1+\sin(0.4t) \\ 1+\sin(0.4t) \\ 1+\sin(0.4t) \end{bmatrix} \times 10^5 N.m, \tag{42}$$

$$\Lambda_x = \begin{cases} 1, \\ 0.75 + 0.1\sin(0.5t + \pi/3) \end{cases}, \tag{43}$$

$$\Lambda_y = \begin{cases} 1, \\ 0.5 + 0.1\sin(0.5t + 2\pi/3) \end{cases}, \tag{44}$$

$$\Lambda_z = \begin{cases} 1, \\ 0.6 + 0.1\sin(0.5t + \pi) \end{cases}. \tag{45}$$

In the simulation, fault Λ is exerted at 6 s and bias fault F_δ is introduced at 9 s. The unmatched disturbance Δf in (3) is assumed to be 0 in the first test, so that no estimation of state X_2 is needed. The parameters for the sliding manifold are set as $k_1 = [1.1,\ 1.1,\ 1.1]$, $k_2 = [4,\ 4,\ 4]$, $a_1 = [1.1,\ 1.1,\ 1.1]$, $a_2 = [3,\ 3,\ 3]$. For the A2-NFTSMC scheme in (22)–(25), the parameters are set as $k_3 = [1.2,\ 1.2,\ 1.2]$, $k_4 = [1.2,\ 1.2,\ 1.2]$, $c_1 = 0.5$, $c_2 = 1.2$, $r = [1,\ 1,\ 1]$, $l_0 = [30,\ 30,\ 30]$, $m_1 = [0.6,\ 0.6,\ 0.6]$, $m_1 = [1.2,\ 1.2,\ 1.2]$, and τ in (40) is chosen as the simulation sample step.

For the NFTSMC, the controller is expressed as

$$u_i = -F_i - k_{1i}a_{1i}\,|x_{1i}|^{a_{1i}-1}\left(\frac{\phi_i}{k_{1i}} + x_{2i}\right) - k_{3i}sign^{c_1}(S_i) - k_{4i}sign^{c_2}(S_i) + k_{5i}sign(S_i), \tag{46}$$

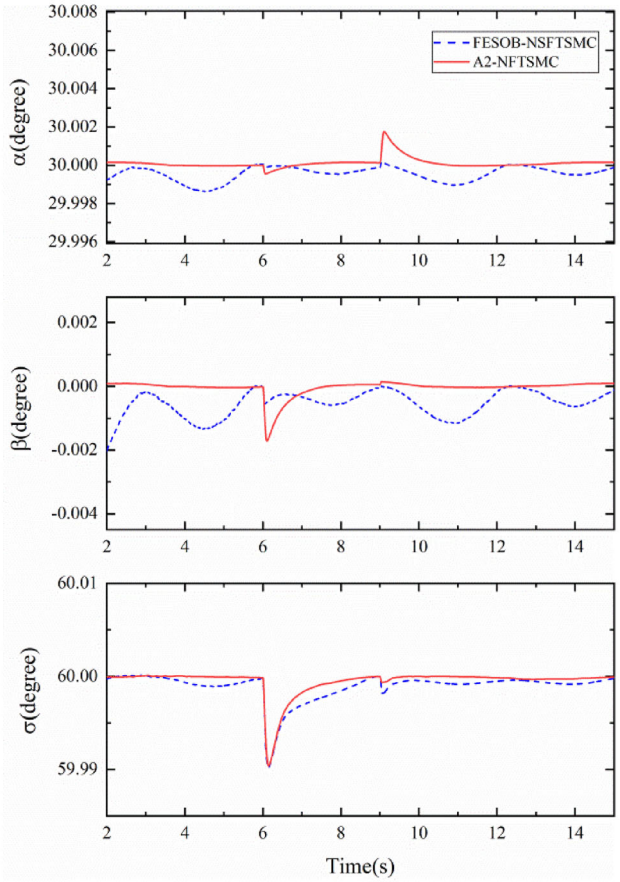

Fig. 5 Comparison of angle of attack, sideslip angle and bank angle between FESOB–NSFTSMC and proposed controller (zoomed)

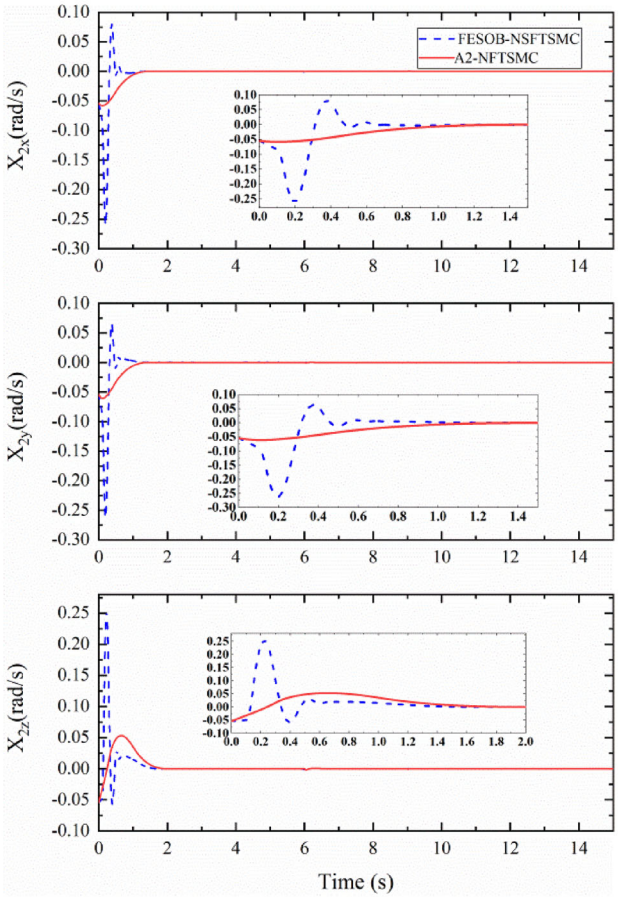

Fig. 6 Comparison of convergence of X_2 between FESOB–NSFTSMC and proposed controller

with $k_5 = [1,\ 1,\ 1]$ and the other parameters are the same as for the A2-NFTSMC. We notice that the NFTSMC is discontinuous and, to set the values of parameters k_5, the upper bounds of ΔD_i must be known in advance. Since using the sign function in (46) can give rise to unacceptably large chattering, the sign function $sign(S_i)$ is often substituted by the function:

$$\varpi_i = \frac{e^{\rho S_i} - 1}{e^{\rho S_i} + 1},\ \ \rho > 0,\ \ i = x,\ y,\ z. \tag{47}$$

In this test, ρ is chosen as 1000. The results of simulation test1 are demonstrated in Figs. 1, 2 and 3. As shown in Fig. 1, both controllers enforce the attitude angles to track the command in finite time. However, the tracking precision of the proposed controller is much superior to that of the NFTSMC, which indicates that the proposed controller exhibits better robustness. In addition, the proposed controller is much less influenced by the actuator faults introduced at 6 s and 9 s, respectively. This also can be observed in Fig. 2, where the controllers drive the state vector X_2 to the origin. The reason for the difference between the performances of the proposed controller and the NFTSMC is that there has to be a tradeoff between the control accuracy and the chattering reduction for the parameter selection of the NFTSMC. In contrast, for the proposed controller, as it represents a higher order control strategy and it is inherently continuous, both chattering reduction and control precision can be guaranteed simultaneously. It can also be observed in Fig. 3 that the proposed control strategy does not produce a very large control torque magnitude at the initial phase as the NFTSMC does. The initial output value of the traditional NFTSMC is sensitive to changes of k_{5i}, i.e., a small rise of the value of k_{5i} can lead to a large increase of the control torque value. The proposed controller eliminates this sensitivity. This feature is very beneficial in real applications when the magnitude of the controller output signal should not surpass the controller's saturation value.

Up to now, the discussion was based on the situation when the state vector X_2 is obtainable. This is not practical in real applications as $\dot{\Omega}$ contains an unknown part Δf. In the second simulation test, Δf is taken into account:

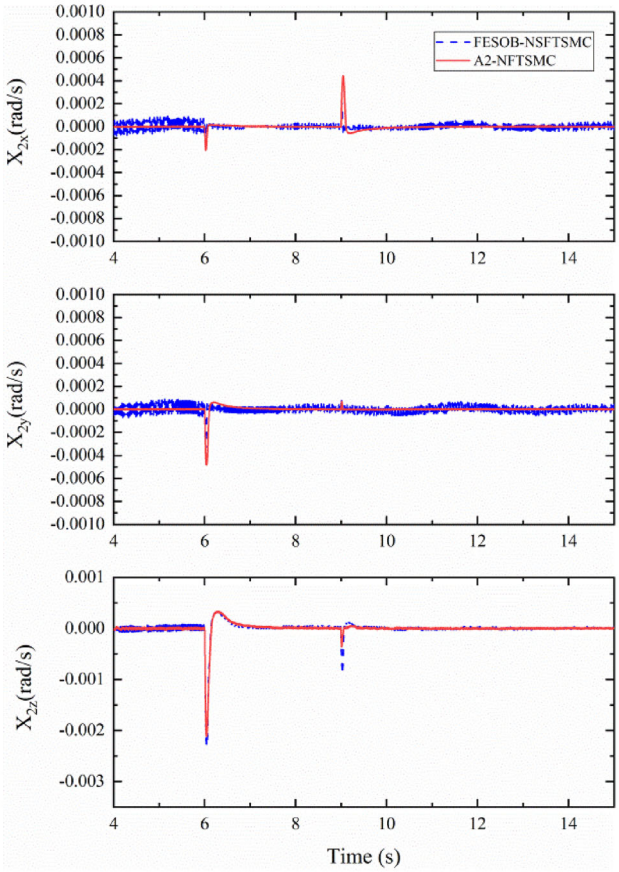

Fig. 7 Comparison of convergence of X_2 between FESOB–NSFTSMC and proposed controller (zoomed)

$$\Delta f = \begin{bmatrix} -\sin(t+0.57) \\ -\sin(t+0.57) \\ -\sin(t+0.57) \end{bmatrix} N \cdot m. \tag{48}$$

The fixed-time extended state observer based non-singular fast terminal sliding mode controller (FESOB–NSFTSMC) in reference [31] is implemented for comparison purposes. The observer and controller of the FESOB–NSFTSMC can be expressed as

$$\begin{aligned} \dot{Z}_1 &= Z_2 + e^{\eta+b}\upsilon sign^{\alpha_1}(X_1 - Z_1) \\ &\quad + e^{\eta+b}(1-\upsilon)sign^{\beta_1}(X_1 - Z_1), \\ \dot{Z}_2 &= Z_3 + e^{2\eta+b}\upsilon\, sign^{\alpha_2}(X_1 - Z_1) \\ &\quad + e^{2\eta+b}(1-\upsilon)sign^{\beta_2}(X_1 - Z_1) + U, \\ \dot{Z}_3 &= e^{3\eta+b}\upsilon\, sign^{\alpha_3}(X_1 - Z_1) + e^{3\eta+b}(1-\upsilon) \\ &\quad sign^{\beta_3}(X_1 - Z_1) + \Upsilon sign(X_1 - Z_1), \end{aligned} \tag{49}$$

$$\upsilon = \begin{cases} 0, & \text{if } t < T_u \\ 1, & \text{if } t > T_u \end{cases}, \tag{50}$$

and

$$\begin{aligned} u_i = &-F_i - k_{1i}a_{1i}\,|x_{1i}|^{a_{1i}-1}\left(\frac{\phi_i}{k_{1i}} + z_{2i}\right) - k_{3i}sign^{c_1}(S_i) \\ &- k_{4i}sign^{c_2}(S_i) - z_{3i}, \quad i = x,\ y,\ z, \end{aligned} \tag{51}$$

where $Z_1 = [z_{1x}, z_{1y}, z_{1z}]$, $Z_2 = [z_{2x}, z_{2y}, z_{2z}]$, $Z_3 = [z_{3x}, z_{3y}, z_{3z}]$, $T_u = 0.1$, $\alpha_1 = 0.8$, $\beta_1 = 1.8$, $\eta = 1.5$, $b = 1.4$ and $\Upsilon = 1$. ϕ_i and S_i have the same form and parameters as in (20) and (24), only with the element x_{2i} substituted by z_{2i}. It is worth noting that, although knowledge of the disturbance bounds is not required for the controller as stated in reference [31], the upper bounds must indeed be known in advance for the design of parameter Υ in the observer. Therefore, the FESOB–NSFTSMC strategy still does not avoid the necessity to learn the disturbance bounds.

For the proposed controller, the parameters are selected as the same as in test 1. Instead of using state or disturbance observers, a time-delay estimation (TDE) scheme is applied to estimate X_2. The benefit of the TDE is its simplicity and straight-forwardness in applications [41, 42]. Here, the TDE scheme is designed as follows.

Integrating both sides of equation $\dot{\Omega} = R\omega + \Delta f$ yields

$$h(t) = \int_0^t \Delta f\, \mathrm{d}\tau = \Omega - \Omega(0) - \int_0^t R\omega \mathrm{d}\tau. \tag{52}$$

The estimation of Δf, $\Delta \hat{f}$, then can be calculated as

$$\Delta \hat{f} = (h(t) - h(t-\tau_0))/\tau_0, \tag{53}$$

where τ_0 is a short time delay that is chosen as the simulation sample step. The estimation of X_2 is further deduced as

$$\hat{X}_2 = R\omega - \dot{\Omega}_{ref} + \Delta \hat{f}. \tag{54}$$

The results of simulation test 2 can be found in Figs. 4, 5, 6, 7 and 8. From Fig. 4, we can see that both controllers have similar fault tolerances and the convergence times of the angles are the same. However, Fig. 5 (the zoomed version of Fig. 4) further illustrates that the proposed controller causes better tracking precision. From Figs. 6 and 7, it is obvious that the proposed controller does not cause large oscillations in the initial stage as the FESOB–NSFTSMC does. Furthermore, it does not cause as much chattering as the latter during the stable phase. The superiority of the proposed controller over the FESOB–NSFTSMC can also be observed from Fig. 8. The control torque of the FESOB–NSFTSMC suffers large oscillations during the initial stage compared with the proposed controller. Although the FESOB–NSFTSMC is also a continuous controller, there has

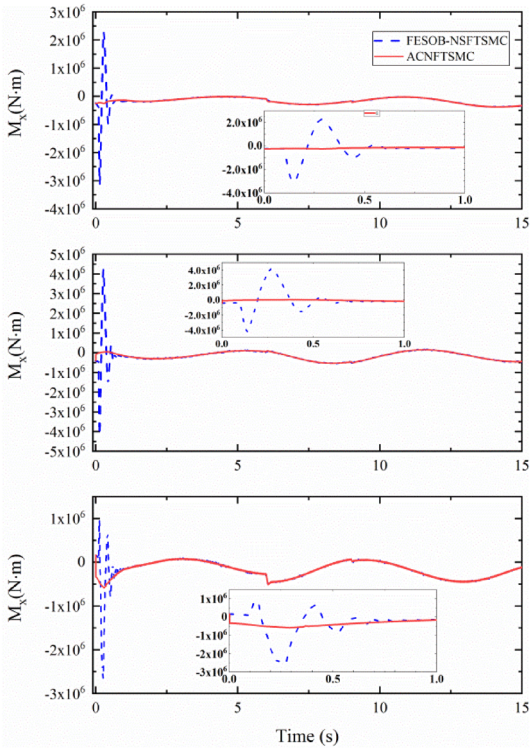

Fig. 8 Comparison of control torque between FESOB–NSFTSMC and proposed controller

to be an observer to estimate the disturbance ΔD. In contrast, the adaptive strategy of the proposed method enables the controller to dominate the disturbances without requiring additional control effort.

5 Conclusions

In this paper, an A2-NFTSMC is proposed as the fault tolerant attitude control scheme for RLVs during their reentry phase. The proposed controller is established based on the NFTSMC which exhibits a fast/fixed-time convergence. By resorting to an adaptive second-order sliding mode control strategy, the traditional discontinuous term of the NFTSMC is avoided and the chattering is reduced, while the robustness of the controller is increased. The upper bounds of the disturbances are no longer needed to be known in advance. Moreover, the newly proposed NFTSMC output value is no longer sensitive to changes of the magnitude of the disturbance as the traditional NFTSMC. Simulation results demonstrate that, compared with the existing NFTSMC based controllers, the proposed one has better robustness and causes less chattering, while its control structure is kept simple and concise.

Acknowledgements This work was supported in part by National Natural Science Foundation of China under Grant No. 62003264, Natural Science Foundation of Shaanxi Province, China under Grant No. 2019ZY-CXPT-03-02 and China Scholarship Council (201606290287).

Declarations

Conflict of interest On behalf of all authors, the corresponding author states that there is no conflict of interest.

References

1. Gao Z et al (2012) Active fault tolerant control design for reusable launch vehicle using adaptive sliding mode technique. J Franklin Inst 349(4):1543–1560
2. Dong Q et al (2017) Adaptive disturbance observer-based finite-time continuous fault-tolerant control for reentry RLV. Int J Robust Nonlinear Control 27(18):4275–4295
3. Yu X, Jiang J (2015) A survey of fault-tolerant controllers based on safety-related issues. Annu Rev Control 39:46–57
4. Zhang Y, Tang S, Guo J (2017) Adaptive-gain fast super-twisting sliding mode fault tolerant control for a reusable launch vehicle in reentry phase. ISA Trans 71:380–390
5. Gao M, Yao J (2018) Finite-time H∞ adaptive attitude fault-tolerant control for reentry vehicle involving control delay. Aerosp Sci Technol 79:246–254
6. Gao M-Z, Cai G-P, Nan Y (2016) Robust adaptive fault-tolerant H∞ control of reentry vehicle considering actuator and sensor faults based on trajectory optimization. Int J Control Autom Syst 14(1):198–210
7. Yu Z et al (2020) Decentralized fractional-order backstepping fault-tolerant control of multi-UAVs against actuator faults and wind effects. Aerosp Sci Technol 104:105939
8. Chen F et al (2016) Robust backstepping sliding-mode control and observer-based fault estimation for a quadrotor UAV. IEEE Trans Industr Electron 63(8):5044–5056
9. Shtessel Y, Hall C, Jackson M (2000) Reusable launch vehicle control in multiple-time-scale sliding modes. J Guid Control Dyn 23(6):1013–1020
10. Liang X et al (2020) Fixed-time observer based fault tolerant attitude control for reusable launch vehicle with actuator faults. Aerosp Sci Technol 107:106314
11. Yu X, Man Z (1996) Model reference adaptive control systems with terminal sliding modes. Int J Control 64(6):1165–1176
12. Zhihong M, Paplinski AP, Wu HR (1994) A robust MIMO terminal sliding mode control scheme for rigid robotic manipulators. IEEE Trans Autom Control 39(12):2464–2469
13. Wu Y, Yu X, Man Z (1998) Terminal sliding mode control design for uncertain dynamic systems. Syst Control Lett 34(5):281–287
14. Zhihong M, Yu XH (1997) Terminal sliding mode control of MIMO linear systems. IEEE Trans Circuits Syst I Fund Theory Appl 44(11):1065–1070
15. Feng Y, Yu X, Han F (2013) On nonsingular terminal sliding-mode control of nonlinear systems. Automatica 49(6):1715–1722
16. Feng Y, Yu X, Man Z (2002) Non-singular terminal sliding mode control of rigid manipulators. Automatica 38(12):2159–2167
17. Yu X, Man Z (2000) Fast terminal sliding mode control for single input systems. In: Proceedings of 2000 Asian Control Conference, Shanghai, China
18. Yu X, Zhihong M (2002) Fast terminal sliding-mode control design for nonlinear dynamical systems. IEEE Transs Circuits Syst I Fund Theory Appl 49(2):261–264

19. Li H, Cai Y (2017) On SFTSM control with fixed-time convergence. IET Control Theory Appl 11(6):766–773
20. Yang L, Yang J (2011) Nonsingular fast terminal sliding-mode control for nonlinear dynamical systems. Int J Robust Nonlinear Control 21(16):1865–1879
21. Zuo Z (2014) Non-singular fixed-time terminal sliding mode control of non-linear systems. IET Control Theory Appl 9(4):545–552
22. Chen Q et al (2018) Adaptive nonsingular fixed-time attitude stabilization of uncertain spacecraft. IEEE Trans Aerosp Electron Syst 54(6):2937–2950
23. Bhat SP, Bernstein DS (2005) Geometric homogeneity with applications to finite-time stability. Math Control Signals Syst 17(2):101–127
24. Edwards C, Shtessel Y (2019) Enhanced continuous higher order sliding mode control with adaptation. J Franklin Inst 356(9):4773–4784
25. Li P et al (2017) Adaptive multivariable integral TSMC of a hypersonic gliding vehicle with actuator faults and model uncertainties. IEEE/ASME Trans Mechatron 22(6):2723–2735
26. Yu X, Li P, Zhang Y (2017) The design of fixed-time observer and finite-time fault-tolerant control for hypersonic gliding vehicles. IEEE Trans Industr Electron 65(5):4135–4144
27. Rabiee H, Ataei M, Ekramian M (2019) Continuous nonsingular terminal sliding mode control based on adaptive sliding mode disturbance observer for uncertain nonlinear systems. Automatica 109:108515
28. Tang P et al (2020) An integral TSMC-based adaptive fault-tolerant control for quadrotor with external disturbances and parametric uncertainties. Aerosp Sci Technol 109:106415
29. Qiao J et al (2019) Composite nonsingular terminal sliding mode attitude controller for spacecraft with actuator dynamics under matched and mismatched disturbances. IEEE Trans Ind Inf 16(2):1153–1162
30. Yang J et al (2013) Continuous nonsingular terminal sliding mode control for systems with mismatched disturbances. Automatica 49(7):2287–2291
31. Zhang L et al (2018) Fixed-time extended state observer based nonsingular fast terminal sliding mode control for a VTVL reusable launch vehicle. Aerosp Sci Technol 82:70–79
32. Zhang L et al (2019) Adaptive fault-tolerant control for a VTVL reusable launch vehicle. Acta Astronaut 159:362–370
33. Hu H et al (2020) Active fault-tolerant attitude tracking control with adaptive gain for spacecrafts. Aerosp Sci Technol 98:105706
34. Van M, Ge SS, Ren H (2016) Finite time fault tolerant control for robot manipulators using time delay estimation and continuous nonsingular fast terminal sliding mode control. IEEE Trans Cybern 47(7):1681–1693
35. Van M (2018) An enhanced robust fault tolerant control based on an adaptive fuzzy PID-nonsingular fast terminal sliding mode control for uncertain nonlinear systems. IEEE/ASME Trans Mechatron 23(3):1362–1371
36. Tian B, Yin L, Wang H (2015) Finite-time reentry attitude control based on adaptive multivariable disturbance compensation. IEEE Trans Industr Electron 62(9):5889–5898
37. Tian B et al (2013) Quasi-continuous high-order sliding mode controller design for reusable launch vehicles in reentry phase. Aerosp Sci Technol 28(1):198–207
38. Lee KW, Singh SN (2014) Robust higher-order sliding-mode finite-time control of aeroelastic systems. J Guid Control Dyn 37(5):1664–1671
39. Basin M (2019) Finite-and fixed-time convergent algorithms: design and convergence time estimation. Annu Rev Control 48:209–221
40. Hardy GH, Littlewood JE, Pólya G (1988) Inequalities. University Press, Cambridge
41. Kali Y et al (2018) Super-twisting algorithm with time delay estimation for uncertain robot manipulators. Nonlinear Dyn 93(2):557–569
42. Wang Y et al (2020) Adaptive time-delay control for cable-driven manipulators with enhanced nonsingular fast terminal sliding mode. IEEE Trans Ind Electron 68(3):2356–2367